

Ferrocene Acidity and C–H Bond Dissociation Energy via Experiment and Theory[#]

Published as part of *The Journal of Physical Chemistry* virtual special issue “*Leo Radom Festschrift*”.

Brent Speetzen[†] and Steven R. Kass*[‡]

Department of Chemistry, University of Minnesota, Minneapolis, Minnesota 55455, United States

Supporting Information

ABSTRACT: The gas-phase acidity of ferrocene ($\Delta H^\circ_{\text{acid}}(1) = 391.5 \pm 1.3 \text{ kcal mol}^{-1}$) and electron affinity of the ferrocenyl radical ($\text{EA}(1\text{r}) = 1.74 \pm 0.08 \text{ eV}$) were measured in a Fourier transform mass spectrometer and combined in a thermodynamic cycle with the known ionization energy of the hydrogen atom to afford the C–H bond dissociation energy of 1 ($\text{BDE}(1) = 118.0 \pm 2.3 \text{ kcal mol}^{-1}$). Companion M06-2X but not B3LYP computations reproduce each of these thermodynamic quantities and are in accord with an unusually strong aromatic C–H BDE. Natural population analysis and atomic polar tensor charges indicate that a covalent description of ferrocene with a neutral iron atom is a better representation of this compound than an ionic one with a doubly charged Fe^{2+} center. Predicted structural differences upon deprotonation of MCp_2 , $\text{M} = \text{Fe}$ and Mg , are also in accord with this view.



$$\Delta H^\circ_{\text{acid}} = 391.5 \pm 1.3 \text{ kcal mol}^{-1} \quad \text{EA} = 40.1 \pm 1.9 \text{ kcal mol}^{-1}$$
$$\text{BDE} = 118.0 \pm 2.3 \text{ kcal mol}^{-1}$$

INTRODUCTION

Ferrocene (FeCp_2 , 1) was first reported by Kealy and Pauson in 1951, and its sandwich structure was correctly assigned the following year.^{1–5} This led to the development, characterization, and investigation of the class of compounds now known as metallocenes. Over the intervening years, these species were extensively studied for a wide variety of uses spanning from a fuel additive for diesel engines⁶ to medical applications given the antianemic and cytotoxic properties of 1.^{7,8} This led to the incorporation of ferrocene into the anticancer drug tamoxifen and has resulted in the ferrocifen family, which consists of six groups and about 200 compounds.^{9–12} Ferrocene derivatives also have been used in areas ranging from biological sensors¹³ and materials chemistry to organic synthesis and asymmetric catalysis.^{14–16} Despite all of these efforts, relatively few investigations addressing the energetics of these species have been carried out.

Ferrocene is commonly used as a reference electrode in electrochemical measurements because it readily undergoes reversible one-electron oxidation to the ferrocenium ion (1^+ , $E_{1/2} = 624 \text{ mV}$ in CH_3CN).¹⁷ Polarographic reduction potential determinations of R_2Hg , RHgCl , and $\text{CpFe}(\text{CO})_2\text{R}$ led Dembovich and Gubin to suggest that ferrocene is more acidic than benzene, and by using Streitwieser and Perrin-type

H bond dissociation energy (BDE) to the best of our knowledge has not been experimentally determined.

In the gas phase, the ionization energy ($6.82 \pm 0.08 \text{ eV}$),²¹ proton affinity ($207 \pm 1 \text{ kcal mol}^{-1}$),²² and homolytic $\text{CpFe}-\text{Cp}$ BDE ($91 \pm 3 \text{ kcal mol}^{-1}$)²³ of 1 have been reported. More recently, the adiabatic detachment energies (ADEs) of mono- and doubly deprotonated 1,1'-ferrocenedicarboxylic acid were measured by Wang and Wang et al.,²⁴ and the vertical detachment energy (VDE) of the conjugate base of ferrocene (1.79 eV) was reported by Bowen et al.²⁵ In this work, the gas-phase acidity ($\Delta H^\circ_{\text{acid}}$) of ferrocene and the electron affinity (EA) of the ferrocenyl radical (CpFeC_5H_4 , 1r) are reported and combined in a thermodynamic cycle to afford the C–H BDE of 1. These experimental determinations are compared to B3LYP and M06-2X computations, and the ionic (1i) vs covalent (1c) nature of ferrocene (Figure 1) is briefly addressed.

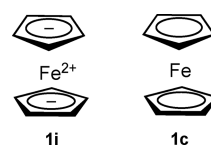


Figure 1. Commonly provided representations of ferrocene corresponding to ionic (1i) and covalent (1c) bonding descriptions.

Received: May 8, 2019

Revised: June 20, 2019

Published: June 21, 2019

EXPERIMENTAL SECTION

Mass Spectrometry. A previously described dual-cell Fourier transform mass spectrometer outfitted with a 3 T superconducting magnet and operated with Ionspec's Omega version 8.0.325 software package was employed for this work.²⁶ Anionic bases corresponding to the conjugate acids of ammonia, diethylamine, dimethylamine, pyrazine, and water were generated by 7.0–8.3 eV electron ionization of these compounds at static pressures. The desired anions were mass isolated using a stored-waveform inverse Fourier transform (SWIFT) excitation²⁷ and transferred to the second cell of the instrument where they were allowed to react with a static pressure of $\sim 2\text{--}9 \times 10^{-8}$ Torr of ferrocene. The resulting ferrocenyl anion was thermally cooled with a $\sim 10^{-5}$ Torr pulse of argon followed by a 1000 ms delay before product ions were ejected and subsequent reactions were monitored. Alternatively, ferrocenyl anion was generated in the first cell by chemical ionization of a mixture of a constant pressure of ferrocene ($\sim 2\text{--}9 \times 10^{-8}$ Torr) and a pulse of ammonia up to a pressure of $\sim 1 \times 10^{-6}$ Torr. The resulting $(\text{M}-\text{H}^+)^-$ ion at m/z 185 was isolated with a SWIFT excitation and transferred to the second cell where it was cooled with an argon pulse. Its reactions with static pressures ($\sim 2\text{--}9 \times 10^{-8}$ Torr) of neutral reagents were subsequently monitored as a function of time. Observed rate constants obtained from these data were uncorrected for pressure differentials that sometimes exist between the reaction region and the ionization gauge.

Computational Methods. Geometries were initially optimized using Gaussian 2003²⁸ with the B3LYP density functional method and the 6-31+G(d) basis set.^{29,30} Vibrational frequencies were subsequently computed for each stationary point, and they all were found to correspond to energy minima and transition structures with zero and one imaginary modes, respectively. Gaussian 2016³¹ was employed to carry out analogous M06-2X optimizations and vibrational frequency determinations with both the aug-cc-pVDZ and aug-cc-pVTZ basis sets.^{32–34} Natural population³⁵ and atomic polar tensor³⁶ analyses were carried out on the latter structures, and all of the acidities, EAs, and BDEs are given as enthalpies at 298 K. Unscaled vibrational frequencies were used in this regard, and small modes that contribute more than 0.5RT to the thermal energy were replaced by 0.5RT. For the BDE computations, the experimental ionization energy of hydrogen (313.6 kcal mol⁻¹) was employed. VDEs were computed from the EAs by replacing the electronic energies for the optimized structures of the radicals with those obtained for the radicals using the anion geometries.

RESULTS

The gas-phase acidity ($\Delta H^\circ_{\text{acid}}$) of ferrocene was measured by reacting it and its conjugate base with a series of standard reference acids and bases to observe the occurrence or nonoccurrence of proton transfer (eq 1). Pyrazide anion ($\Delta H^\circ_{\text{acid}} = 392.6 \pm 2.5$ kcal mol⁻¹) and stronger bases were deprotonate ferrocene, whereas hydroxide ($\Delta H^\circ_{\text{acid}} = 390.33 \pm 0.01$ kcal mol⁻¹) did not.³⁷ Likewise, the Trial Version found to protonate the conjugate base of ferrocene, but weaker acids did not. These bracketing results, summarized in Table 1, enable us to assign $\Delta H^\circ_{\text{acid}} = 391.5 \pm 1.3$ kcal mol⁻¹ for the acidity of ferrocene.^{38–41}

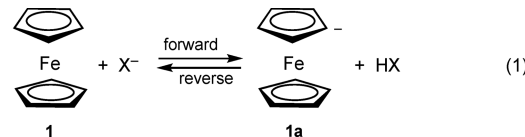


Table 1. Bracketing Results for the Acidity of Ferrocene in kcal mol⁻¹

acid (HX)	$\Delta H^\circ_{\text{acid}}$	proton transfer	
		forward	reverse
NH ₃	403.4 \pm 0.3	yes	no
CH ₃ CH ₂ NH ₂	399.3 \pm 1.1	yes	no
(CH ₃) ₂ NH	396.4 \pm 0.9	yes	no
pyrazine	392.6 \pm 2.5	yes ^a	no
H ₂ O	390.33 \pm 0.01	no	yes ^b

^a $k = 7.1 \times 10^{-10}$ cm³ molecule⁻¹ s⁻¹ ($k_{\text{ADO}} = 1.32 \times 10^{-9}$ cm³ molecule⁻¹ s⁻¹, 54% efficiency); 17.7 Å³ (from the M06-2X/aug-cc-pVTZ calculation) was used for the polarizability. ^b $k = 1.0 \times 10^{-9}$ cm³ molecule⁻¹ s⁻¹ ($k_{\text{ADO}} = 1.75 \times 10^{-9}$ cm³ molecule⁻¹ s⁻¹, 57% efficiency).

Analogous electron transfer reactions were carried out on the ferrocenyl anion (1a) with a series of reference compounds with known EAs to determine the EA of the ferrocenyl radical (1r). Our results are summarized in Table 2,

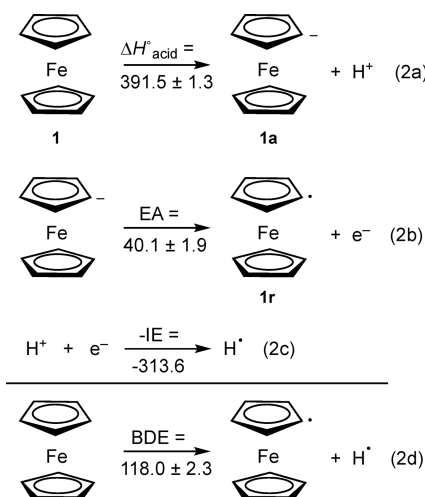
Table 2. Bracketing Results for the EA of Ferrocenyl Radical in eV

cmpd	EA	electron transfer
C ₆ H ₅ NO ₂	1.00 \pm 0.01	no
3-FC ₆ H ₄ NO ₂	1.24 \pm 0.10	no
2-CF ₃ C ₆ H ₄ NO ₂	1.33 \pm 0.10	no
3-CF ₃ C ₆ H ₄ NO ₂	1.41 \pm 0.10	no
(C ₆ F ₅) ₂ CO	1.52 \pm 0.11	no
4-O ₂ NC ₆ H ₄ CHO	1.691 \pm 0.087	no
3,5-(CF ₃) ₂ C ₆ H ₃ NO ₂	1.79 \pm 0.10	yes ^b
1,4-C ₆ H ₄ O ₂ ^a	1.860 \pm 0.005	yes ^c

^a1,4-Benzoquinone. ^b $k = 4.79 \times 10^{-9}$ cm³ molecule⁻¹ s⁻¹ ($k_{\text{ADO}} = 1.14 \times 10^{-9}$ cm³ molecule⁻¹ s⁻¹); $\mu_D = 1.93$ D and $\alpha = 14.8$ Å³ were used. A small amount ($\sim 10\%$) of an adduct anion was also observed. ^c $k = 2.44 \times 10^{-9}$ cm³ molecule⁻¹ s⁻¹ ($k_{\text{ADO}} = 9.27 \times 10^{-10}$ cm³ molecule⁻¹ s⁻¹). A small amount ($\sim 15\%$) of deprotonation was also observed.

and because 1a does not undergo electron transfer with *p*-nitrobenzaldehyde (EA = 1.691 \pm 0.087 eV) but does transfer an electron to 3,5-bis(trifluoromethyl)nitrobenzene (EA = 1.79 \pm 0.10 eV), we assign EA(1r) = 1.74 \pm 0.08 eV (40.1 \pm 1.9 kcal mol⁻¹). This value is nearly the same as the VDE of 1.79 eV reported by Bowen et al.²⁵ and reveals that the ADEs and VDEs are similar for this radical.

The C–H BDE for ferrocene can be determined by combining the acidity and EA measurements above in a thermodynamic cycle as shown in eq 2, where all of the values are given in kcal mol⁻¹. A BDE of 118.0 \pm 2.3 kcal mol⁻¹ is obtained for this quantity, and this value is 5–6 kcal mol⁻¹ larger than the bond energies for benzene (113.5 \pm 0.5 kcal mol⁻¹)⁴² and naphthalene (112.2 \pm 1.2 (α) and 111.9 \pm 1.4 (β) kcal mol⁻¹).⁴³ This result is also in accord with previous reports that phenyl and alkyl radicals do not abstract a



hydrogen atom from **1**,^{19,20} as well as a previously computed BDE of 117.6 kcal mol⁻¹ at 0 K.⁴⁴

B3LYP calculations with the 6-31+G(d) basis set were carried out on ferrocene, the ferrocenyl anion, and its corresponding radical. All three species were found to prefer an eclipsed conformation, and their geometries are provided in the Supporting Information. Energetic quantities are given at 298 K and are summarized in Table 3. Given the poor agreement between the experimental and computed EA of **1r** (or equivalently the ADE of **1a**) and the C–H BDE of **1**, additional M06-2X computations were carried out with the aug-cc-pVDZ and aug-cc-pVTZ basis sets. There are few differences in the M06-2X/aug-cc-pVDZ and M06-2X/aug-cc-pVTZ structures and energetics; therefore, only the latter geometries are illustrated in Figure 2. All of the computed M06-2X thermodynamic quantities, however, are provided in Table 3. Likewise, computed M06-2X/aug-cc-pVTZ charges and spin densities are provided for **1**, **1a**, and **1r** in Table 4.

DISCUSSION

Measured electrochemical reduction potentials of organomercury and cyclopentadienyliron dicarbonyl derivatives in different solvents (i.e., 90% dioxane, dimethylformamide, and acetonitrile) by Denisovich and Gubin led to correlations with dimethyl sulfoxide $\text{p}K_a$ values that resulted in an acidity for ferrocene of $38-40 \pm 3$.¹⁸ This indicates that **1** is more acidic than benzene because the latter compound has a reported $\text{p}K_a$ of 43.0 ± 0.2 .⁴⁵ In accord with these liquid-phase estimates, our determination of $\Delta H^\circ_{\text{acid}}(1) = 391.5 \pm 1.3$ kcal mol⁻¹ reveals that ferrocene is more acidic in the gas phase than benzene ($\Delta H^\circ_{\text{acid}} = 401.7 \pm 0.5$ kcal mol⁻¹)⁴² and naphthalene (394.2 ± 1.2 and 395.5 ± 1.3 kcal mol⁻¹ for the α and β positions, respectively).⁴³ The latter compound is

used as a point of comparison because it is an aromatic hydrocarbon with the same number of carbon atoms as **1**. Our acidity determination is also well reproduced by M06-2X/aug-cc-pVDZ and M06-2X/aug-cc-pVTZ predictions of 392.6 and 393.7 kcal mol⁻¹, respectively.

One might naively assume that the acidity of ferrocene can be used to distinguish between the ionic and covalent bonding descriptions for this compound in that the former bonding view should lead to a less acidic compound due to charge repulsion between the negatively charged cyclopentadienide ring and the carbanion center formed upon deprotonation. The covalent bonding model for ferrocene is reminiscent of an aromatic benzene ring, but because **1** has the same number of carbon atoms as naphthalene, one might expect it to be more acidic than benzene and similar to naphthalene. Our measured value indicates that **1** is 10 kcal mol⁻¹ more acidic than benzene and 3–4 kcal mol⁻¹ more acidic than naphthalene. This seems to suggest that **1c** is a better description of ferrocene than **1a**, and in accord with this view, the computed M06-2X/aug-cc-pVTZ Mulliken, atomic polar tensor (APT), and natural population analysis (NPA) charges on the iron in **1** and **1a** are close to zero (i.e., -0.03 and -0.02 (Mulliken), -0.16 and -0.15 (APT), and 0.03 and 0.00 (NPA), where the first and second numbers in each pair are for **1** and **1a**, respectively). The real bonding situation, of course, is more complex, and an attractive Coulombic interaction in **1a** between the negatively charged centers and a 2+ iron center in the ionic bonding model cannot be discounted.^{46,47}

To address this issue further, the acidity of bis(cyclopentadienyl)magnesium (MgCp_2) was calculated because Mg is more electropositive than Fe (i.e., the Pauling electronegativities are 1.31 and 1.83, respectively)⁴⁸ and the former does not have occupied d orbitals. Consequently, it seems reasonable to expect that MgCp_2 has more ionic character than FeCp_2 . In accord with this view, the M06-2X/aug-cc-pVTZ APT and NPA charges on Mg are 0.89 and 1.80. An intuitively unreasonable Mulliken charge of -0.49 was also obtained, but this method is well-known to have a number of deficiencies and changes sign with the computational approach (i.e., the B3LYP/6-31+G(d) charge is $+0.50$).⁴⁹ Computed acidities for MgCp_2 of 390.9 (B3LYP/6-31+G(d)), 389.4 (M06-2X/aug-cc-pVDZ), 390.3 (M06-2X/aug-cc-pVTZ//M06-2X/aug-cc-pVDZ), and 390.4 kcal mol⁻¹ (M06-2X/aug-cc-pVTZ) all indicate that this metallocene is a little more acidic than FeCp_2 . This suggests that this thermodynamic quantity is not a reliable indicator of the covalent vs ionic character in these species; however, the structural changes upon proton abstraction are illuminating. That is, upon deprotonation of ferrocene, the Fe–C⁻ distance increases by 0.06 Å, whereas for MgCp_2 , the Mg–C⁻ separation decreases by 0.15 Å. The latter change is in accord

Table 3. Computed Acidities, EAs, VDEs, and BDEs for Ferrocene or Ferrocenyl Radical^a

method	$\Delta H^\circ_{\text{acid}}$	EA ^b	VDE	BDE
B3LYP/6-31+G(d)	394.3	1.42	1.77	113.4
M06-2X/aug-cc-pVDZ	392.6	1.67	1.69	117.6
M06-2X/aug-cc-pVTZ sp ^c	393.7	1.75	1.77	120.3
M06-2X/aug-cc-pVTZ	393.7	1.74	1.77	120.3
	391.5 ± 1.3	1.74 ± 0.08	1.79^d	118.0 ± 2.3

^aAcidities and BDEs are in kcal mol⁻¹, whereas EAs and VDEs are in eV. ^bEA = ADE. ^cM06-2X/aug-cc-pVTZ sp = M06-2X/aug-cc-pVTZ//M06-2X/aug-cc-pVDZ. ^dSee ref 25.

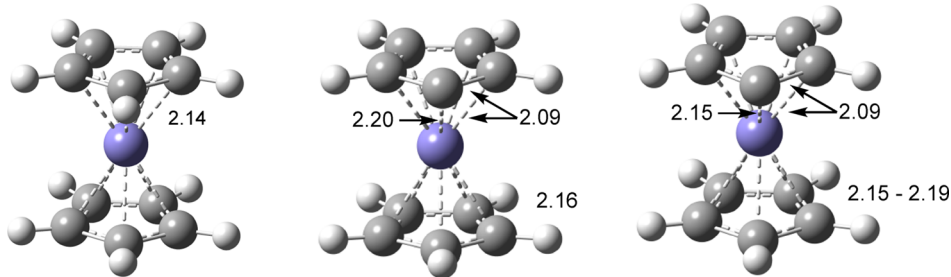


Figure 2. M06-2X/aug-cc-pVTZ optimized geometries of ferrocene (left), ferrocenyl anion (middle), and ferrocenyl radical (right). Fe–C distances are given in Angstroms.

Table 4. Computed Mulliken, Atomic Polar Tensor (APT), and Natural Population Analysis (NPA) Charges and Spin Densities for Ferrocene, Ferrocenyl Anion, and Ferrocenyl Radical^a

cmpd/site	charge			spin density
	Mulliken	APT	NPA	
1				
Fe	−0.03	−0.16	0.03	
C	0.00	0.02	0.00	
1a				
Fe	−0.02	−0.15	0.00	
C [−]	−1.47	−0.44	−0.36	
C–C [−]	0.39	−0.07	−0.14	
C–C–C [−]	−0.06	−0.10	−0.09	
Cp ^b	−0.04 to −0.03	−0.02 to −0.01	−0.05 to −0.02	
1r				
Fe	0.00	0.29	0.27	1.30
C [•]	−1.22	−0.43	−0.24	−0.06
C–C [•]	0.42	0.06	−0.05	−0.03
C–C–C [•]	0.09	0.02	0.00	−0.05
Cp ^b	0.00 to 0.07	−0.02 to 0.01	0.00 to 0.04	−0.02 to −0.01

^aAll values are from M06-2X/aug-cc-pVTZ structures and calculations. ^bRemote cyclopentadienyl ring carbons, all of which fall in the indicated range.

with a predominantly electrostatic interaction that brings the oppositely charged centers closer together. Electron repulsion presumably accounts for the opposite behavior in ferrocene and suggests that covalent bonding is dominant for this compound.^{46,47}

Ferrocenyl anion previously was reported in the gas phase, and its VDE was determined to be 1.79 eV by photoelectron spectroscopy.²⁵ Companion CAM-B3LYP/6-31+G(d,p) computations (1.77 eV) are in excellent accord with this result and led to a prediction of 1.44 eV for the EA of the ferrocenyl radical. Our B3LYP/6-31+G(d) calculations give nearly the same results, but the M06-2X computations indicate that the VDE and EA are nearly equal and reproduce the experimental determinations for both of these quantities. Given the similar geometries of **1a** and **1r**, it is not surprising that the VDE and EA are almost the same. Moreover, because ferrocene is more acidic than benzene and naphthalene and five-membered aromatic ring compounds have 5–10 kcal mol^{−1} larger carbon–hydrogen bond energies than six-membered ring species,^{50,51} one would expect **1r** to have a larger EA than

^{16.00 ± 0.006} eV⁴² and both naphthyl radicals (1.30 ± 0.02 (β) and 1.37 ± 0.02 (α) eV).⁴³ A reasonable estimate of the Trial Version of **1r** based upon these acidity and BDE differences is $1.63\text{--}1.98$ eV, which is in excellent accord with the M06-2X predictions of 1.67–1.75 eV and our experimental determination of 1.74 ± 0.08 eV.

The nature of the ferrocenyl radical was also explored. Upon the basis of the APT and NPA **1a**–**1r** charge differences, it is apparent that the loss of an electron from the ferrocenyl anion primarily comes from the iron atom and the π -system. This is in accord with the Mulliken spin density of 1.30 at the Fe center and a plot of the spin density (Figure 3). In contrast, the Mulliken **1a**–**1r** charge differences and the B3LYP/6-31+G(d) results are in accord with a σ -radical. We suspect that the former view provides a better description of

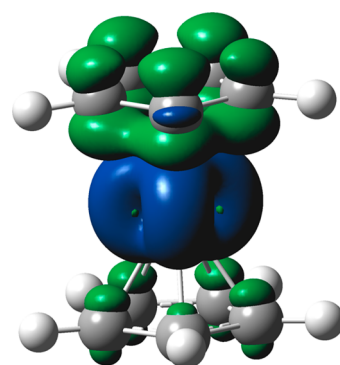


Figure 3. Electron density from the spin density of the ferrocenyl radical (isovalue = 0.002) using the M06-2X/aug-cc-pVTZ optimized geometry.

the ferrocenyl radical, but a spectroscopic investigation of **1r** would be useful.

Our experimentally determined C–H BDE of 118.0 kcal mol^{−1} for ferrocene is 4.5 ± 2.4 kcal mol^{−1} larger than that for benzene and 5.8 ± 2.6 and 6.1 ± 2.7 kcal mol^{−1} larger than those for naphthalene. This unusually large BDE is in accord with liquid-phase observations and is well reproduced by M06-2X computations but not those with the B3LYP density functional. It is also in accord with separate predictions by Hadad et al. and Guo et al. for five-membered aromatic ring compounds, which were found to have larger C–H bond energies than six-membered species.^{50,51} This was reasonably attributed to the smaller C–C–C bond angles in five-membered rings, resulting in additional angle strain in the corresponding radical. Diminished hyperconjugation may also play a role in the large C–H BDE of **1**.

CONCLUSIONS

Ferrocene was found to be more acidic than benzene and naphthalene in the gas phase, and its conjugate base is harder to oxidize than phenyl or naphthyl anions. That is, the EA of the ferrocenyl radical is significantly larger than those for phenyl and both naphthyl radicals. These results are in accord with a relatively stable ferrocene conjugate base and the well-known synthetically useful metalation chemistry of **1** in the liquid phase. These findings are also well reproduced by M06-2X computations and lead to a covalent bonding description of ferrocene rather than an ionic one.

The C–H BDE of ferrocene is significantly larger than the CpFe–Cp ligand bond energy (118.0 ± 2.3 vs 91 ± 3 kcal mol^{−1}) and the carbon–hydrogen BDEs of benzene and naphthalene. This can be attributed to the relatively high energy of the ferrocenyl radical and the greater stability of an aromatic carbon radical in a six-membered ring than in a five-membered one. This also accounts for the dearth of synthetic transformations proceeding through the intermediacy of **1r**.

ASSOCIATED CONTENT

Supporting Information

The Supporting Information is available free of charge on the ACS Publications website at DOI: [10.1021/acs.jpca.9b04382](https://doi.org/10.1021/acs.jpca.9b04382).

Computed structures and energies along with complete citations to refs 28 and 31 (PDF)

AUTHOR INFORMATION

Corresponding Author

*E-mail: kass@umn.edu. Phone: +1 612-625-7513.

ORCID

Steven R. Kass: [0000-0001-7007-9322](https://orcid.org/0000-0001-7007-9322)

Present Address

†B.S.: Department of Chemistry, University of Wisconsin—Stevens Point, Stevens Point, Wisconsin 54481.

Notes

The authors declare no competing financial interest.

The manuscript was taken in part from Speetzen, B., M. S. Thesis, University of Minnesota, 2007.

for Advanced Computational Research is gratefully acknowledged.

REFERENCES

- Kealy, T. J.; Pauson, P. L. A New Type of Organo-Iron Compound. *Nature* **1951**, *168*, 1039–1040.
- Miller, S. A.; Tebboth, J. A.; Tremaine, J. F. Dicyclopentadienyliron. *J. Chem. Soc.* **1952**, *632*–635.
- Wilkinson, G.; Rosenblum, M.; Whiting, M. C.; Woodward, R. B. The Structure of Iron Bis-Cyclopentadienyl. *J. Am. Chem. Soc.* **1952**, *74*, 2125–2126.
- Woodward, R. B.; Rosenblum, M.; Whiting, M. C. A New Aromatic System. *J. Am. Chem. Soc.* **1952**, *74*, 3458–3459.
- Fischer, E. O.; Pfab, W. Z. Cyclopentadien-Metallkomplexe, ein Neuer Typ Metallorganischer Verbindungen. *Z. Naturforsch., B: J. Chem. Sci.* **1952**, *7*, 377–379.
- Bonczyk, P. A. Effect of Ferrocene on Soot in a Prevaporized Iso-octane/Air Diffusion Flame. *Combust. Flame* **1991**, *87*, 233–244.
- Köpf-Maier, P.; Köpf, H. Non-Platinum Group Metal Antitumor Agents. History, Current Status, and Perspectives. *Chem. Rev.* **1987**, *87*, 1137–1152.
- Köpf-Maier, P.; Köpf, H. Transition and Main-Group Metal Cyclopentadienyl Complexes: Preclinical Studies on a Series of Antitumor Agents of Different Structural Type. *Struct. Bonding* **1988**, *70*, 103–185.
- Jaouen, G.; Top, S.; Vessières, A.; Leclercq, G.; Quivy, J.; Jin, L.; Croisy, A. The First Organometallic Antioestrogens and Their Antiproliferative Effects. *C. R. Acad. Sci., Ser. IIc: Chim.* **2000**, *3*, 89–93.
- Top, S.; Vessières, A.; Cabestaing, C.; Laios, I.; Leclercq, G.; Provost, C.; Jaouen, G. Studies on Organometallic Selective Estrogen Receptor Modulators. (SERMS) Dual Activity in the Hydroxy-Ferrocifen Series. *J. Organomet. Chem.* **2001**, *637*–639, 500–506.
- Top, S.; Vessières, A.; Leclercq, G.; Quivy, J.; Tang, J.; Vaissermann, J.; Huché, M.; Jaouen, G. Synthesis, Biochemical Properties and Molecular Modelling Studies of Organometallic Specific Estrogen Receptor Modulators (SERMs), the Ferrocifens and Hydroxyferrocifens: Evidence for an Antiproliferative Effect of Hydroxyferrocifens on both Hormone-Dependent and Hormone-Independent Breast Cancer Cell Lines. *Chem. - Eur. J.* **2003**, *9*, 5223–5236.
- Jaouen, G.; Vessières, A.; Top, S. Ferrocifen Type Anti Cancer Drugs. *Chem. Soc. Rev.* **2015**, *44*, 8802–8817.
- Hale, P. D.; Inagaki, T.; Karan, H. I.; Okamoto, Y.; Skotheim, T. A. A New Class of Amperometric Biosensor Incorporating a Polymeric Electron-Transfer Mediator. *J. Am. Chem. Soc.* **1989**, *111*, 3482–3484.
- Atkinson, R. C. J.; Gibson, V. C.; Long, N. J. The Syntheses and Catalytic Applications of Unsymmetrical Ferrocene Ligands. *Chem. Soc. Rev.* **2004**, *33*, 313–328.
- Gomez Arrayas, R.; Adrio, J.; Carretero, J. C. Recent Applications of Chiral Ferrocene Ligands in Asymmetric Catalysis. *Angew. Chem., Int. Ed.* **2006**, *45*, 7674–7715.
- Ferrocenes: Homogeneous Catalysis, Organic Synthesis, Materials Science; Togni, A., Hayashi, T., Eds.; Wiley-VCH: Weinheim, Germany, 1995.
- Pavlishchuk, V. V.; Addison, A. W. Conversion Constants for Redox Potentials Measured Versus Different Reference Electrodes in Acetonitrile Solutions at 25°C. *Inorg. Chim. Acta* **2000**, *298*, 97–102.
- Denisovich, L. I.; Gubin, S. P. Electrochemical Studies of Organometallic Compounds III. The Polarographic Determination of the C–H Acidity of Metallocenes. *J. Organomet. Chem.* **1973**, *57*, 109–119.
- Beckwith, A. L. J.; Leydon, R. J. The Mechanism of the Reaction of Ferrocene with Free-Radical Reagents. *Tetrahedron Lett.* **1963**, *6*, 385–388.
- Broadhead, G. D.; Pauson, P. L. Ferrocene Derivatives. Part II. Arylation. *J. Chem. Soc.* **1955**, 367–370.



pdfelement

The Trial Version

ACKNOWLEDGMENTS

Generous support from the National Science Foundation (CHE-1665392) and the Minnesota Supercomputer Institute

(21) Ryan, M. F.; Eyler, J. R.; Richardson, D. E. Adiabatic Ionization Energies, Bond Disruption Enthalpies, and Solvation Free Energies for Gas-Phase Metallocenes and Metallocenium Ions. *J. Am. Chem. Soc.* **1992**, *114*, 8611–8619.

(22) Meot-Ner, M. Ion Chemistry of Ferrocene. Thermochemistry of Ionization and Protonation and Solvent Clustering. Slow and Entropy-Driven Proton-Transfer Kinetics. *J. Am. Chem. Soc.* **1989**, *111*, 2830–2834.

(23) Lewis, K. E.; Smith, G. P. Bond Dissociation Energies in Ferrocene. *J. Am. Chem. Soc.* **1984**, *106*, 4650–4651.

(24) Wang, X. B.; Dai, B.; Woo, H. K.; Wang, L. S. Intramolecular Rotation through Proton Transfer: $[\text{Fe}(\eta^5\text{-C}_5\text{H}_4\text{CO}_2^-)_2]$ versus $[(\eta^5\text{-C}_5\text{H}_4\text{CO}_2^-)\text{Fe}(\eta^5\text{-C}_5\text{H}_4\text{CO}_2\text{H})]$. *Angew. Chem., Int. Ed.* **2005**, *44*, 6022–6024.

(25) Ricke, N.; Eustis, S. N.; Bowen, K. H. Combined Experimental and Theoretical Study of Deprotonated Ferrocene: Anion Photoelectron Spectroscopy and Density Functional Calculations. *Int. J. Mass Spectrom.* **2014**, *357*, 63–65.

(26) Reed, D. R.; Hare, M. C.; Kass, S. R. Formation of Gas-Phase Dianions and Distonic Ions As A General Method for the Synthesis of Protected Reactive Intermediates. Energetics of 2,3- and 2,6-Dehydronaphthalene. *J. Am. Chem. Soc.* **2000**, *122*, 10689–10696.

(27) Wang, T. C. L.; Ricca, T. L.; Marshall, A. G. Extension of Dynamic Range in Fourier Transform Ion Cyclotron Resonance Mass Spectrometry via Stored Waveform Inverse Fourier Transform Excitation. *Anal. Chem.* **1986**, *58*, 2935–2938.

(28) Frisch, M. J.; Trucks, G. W.; Schlegel, H. B.; Scuseria, G. E.; Robb, M. A.; Cheeseman, J. R.; Montgomery, J. A., Jr.; Vreven, T.; Kudin, K. N.; Burant, J. C.; et al. *Gaussian 03*, revision D.01; Gaussian, Inc.: Pittsburgh, PA, 2003.

(29) Becke, A. D. Density-Functional Thermochemistry. III. The Role of Exact Exchange. *J. Chem. Phys.* **1993**, *98*, 5648–5652.

(30) Lee, C.; Yang, W.; Parr, R. G. Development of the Colle-Salvetti Correlation-Energy Formula Into A Functional of the Electron Density. *Phys. Rev. B: Condens. Matter Mater. Phys.* **1988**, *37*, 785–789.

(31) Frisch, M. J.; Trucks, G. W.; Schlegel, H. B.; Scuseria, G. E.; Robb, M. A.; Cheeseman, J. R.; Scalmani, G.; Barone, V.; Petersson, G. A.; Nakatsuji, H.; et al. *Gaussian 16*, revision B.01; Gaussian, Inc.: Wallingford, CT, 2016.

(32) Zhao, Y.; Truhlar, D. G. How Well Can New-Generation Density Functionals Describe the Energetics of Bond-Dissociation Reactions Producing Radicals? *J. Phys. Chem. A* **2008**, *112*, 1095–1099.

(33) Zhao, Y.; Truhlar, D. G. The M06 Suite of Density Functionals for Main Group Thermochemistry, Thermochemical Kinetics, Noncovalent Interactions, Excited States, and Transition Elements: Two New Functionals and Systematic Testing of Four M06-Class Functionals and 12 Other Functionals. *Theor. Chem. Acc.* **2008**, *120*, 215–241.

(34) Zhao, Y.; Truhlar, D. G. Density Functionals with Broad Applicability in Chemistry. *Acc. Chem. Res.* **2008**, *41*, 157–167.

(35) Reed, A. E.; Weinstock, R. B.; Weinhold, F. Natural Population Analysis. *J. Chem. Phys.* **1985**, *83*, 735–746.

(36) Cioslowski, J. A. New Population Analysis Based on Atomic Polar Tensors. *J. Am. Chem. Soc.* **1989**, *111*, 8333–8336.

(37) For gas-phase acidities and electron affinities, see: Bartmess, J. E. *NIST Chemistry WebBook, NIST Standard Reference Database Number 69*; Mallard, W. G., Linstrom, P. G.; Eds.; National Institute of Standards and Technology: Gaithersburg, MD, 2018; <http://webbook.nist.gov>.

(38) Collision rates were computed as described in the following reference. See T. J. Bowers, M. T. Ion-Polar Molecule Collisions: The Effect of Ion Size on Ion-Polar Molecule Rate Constants: The Parameterization of the Average-Dipole-Orientation Theory. *Int. J. Mass Spectrom. Ion Phys.* **1973**, *12*, 347–356.

(39) Miller, K. J.; Savchik, J. A. A New Empirical Method to Calculate Average Molecular Polarizabilities. *J. Am. Chem. Soc.* **1979**, *101*, 7206–7213.

(40) For previously computed ferrocene polarizabilities, see: Semwal, R. P.; Uniyal, R. C.; Balodi, J. P. Polarizability of Ferrocene Derivatives Using A New Empirical Approach. *J. Indian Chem. Soc.* **2004**, *81*, 68–70 and ref 41.

(41) Labello, N. P.; Ferreira, A. M.; Kurtz, H. A. Utilizing Relativistic Effective Core Potentials for Accurate Calculations of Molecular Polarizabilities on Transition Metal Compounds. *J. Phys. Chem. A* **2006**, *110*, 13507–13513.

(42) Davico, G. E.; Bierbaum, V. M.; DePuy, C. H.; Ellison, G. B.; Squires, R. R. The C–H Bond Energy of Benzene. *J. Am. Chem. Soc.* **1995**, *117*, 2590–2599.

(43) Reed, D. R.; Kass, S. R. Experimental Determination of the α and β C–H Bond Dissociation Energies in Naphthalene. *J. Mass Spectrom.* **2000**, *35*, 534–539.

(44) Elihn, K.; Larsson, K. A. Theoretical Study of the Thermal Fragmentation of Ferrocene. *Thin Solid Films* **2004**, *458*, 325–329. We estimate that the BDE is 1.5 kcal mol⁻¹ larger at 298 K based upon our M06-2X computations.

(45) Streitwieser, A., Jr.; Scannon, P. J.; Niemeyer, H. M. Acidity of Hydrocarbons. XLIX. Equilibrium Ion Pair Acidities of Fluorinated Benzenes for Cesium Salts in Cyclohexylamine. Extrapolation of pK of Benzene. *J. Am. Chem. Soc.* **1972**, *94*, 7936–7937.

(46) Rayón, V. M.; Frenking, G. Bis(benzene)chromium Is a δ -Bonded Molecule and Ferrocene Is a π -Bonded Molecule. *Organometallics* **2003**, *22*, 3304–3308.

(47) Frunzke, J.; Lein, M.; Frenking, G. Structures, Metal–Ligand Bond Strength, and Bonding Analysis of Ferrocene Derivatives with Group-15 Heteroligands $\text{Fe}(\eta^5\text{-E}_5)_2$ and $\text{FeCp}(\eta^5\text{-E}_5)$ (E = N, P, As, Sb). A Theoretical Study. *Organometallics* **2002**, *21*, 3351–3359.

(48) Pauling, L. *The Nature of the Chemical Bond*, 3rd ed.; Cornell University Press: Ithaca, NY, 1960.

(49) Wiberg, K. B.; Rablen, P. R. Comparison of Atomic Charges Derived via Different Procedures. *J. Comput. Chem.* **1993**, *14*, 1504–1518.

(50) Barckholtz, C.; Barckholtz, T. A.; Hadad, C. M. C–H and N–H Bond Dissociation Energies of Small Aromatic Hydrocarbons. *J. Am. Chem. Soc.* **1999**, *121*, 491–500.

(51) Feng, Y.; Wang, J. T.; Liu, L.; Guo, Q. X. C–H and N–H Bond Dissociation Energies of Five- and Six-membered Ring Aromatic Compounds. *J. Phys. Org. Chem.* **2003**, *16*, 883–890.